applied sciences

MDPI

Article

Effects of Waste Plastic and Glass Aggregates on the Strength Properties of Ambient-Cured One-Part Metakaolin-Based Geopolymer Concrete

Babatunde Luke Ajayi * and Adewumi John Babafemi *

Department of Civil Engineering, Stellenbosch University, Stellenbosch 7602, South Africa
* Correspondence: 26810808@sun.ac.za (B.L.A.); ajbabafemi@sun.ac.za (A.J.B.); Tel.: +27-21-808-4475 (B.L.A.)

Abstract: The production of Portland cement (PC) is associated with carbon emissions. One-part geopolymer "just add water" is a user- and environmentally-friendly binder that can potentially substitute PC. However, there is limited research on the setting time, fresh, and strength properties of one-part metakaolin (MK)-based geopolymer concrete (OMGPC) incorporating recycled aggregates. Hence, the study explored the fresh, mechanical (compressive, flexural, splitting tensile, and E-modulus) and microstructural properties of ambient cured (7-, 28-, and 90-day) OMGPC containing recycled waste plastics (RESIN8) and recycled fine waste glass aggregate (FWG) at 5% and 10% by volume of the sand. The study result shows that 2% trisodium phosphate by wt. of the binder retard the initial and final setting times of OMGPC. At the same time, the incorporation of RESIN8 and FWG aggregates improved the workability of geopolymer concrete. The lightweight properties of RESIN8 aggregate reduce the hardened density of OMGPC, while the FWG specimens show a similar density to the control. The compressive strength of RESIN8 and FWG OMGPC range from 19.8 to 24.6 MPa and 26.9 to 30 MPa, respectively, compared to the control (26 to 28.9 MPa) at all curing ages. The flexural and splitting tensile strength of the OMGPC range from 2.2 to 4.5 MPa and 1.7 to 2.8 MPa, respectively. OMGPC is a viable alternative to Portland cement, and FWG can substitute sand in structural concrete by up to 10% and RESIN8 aggregate at 5% by volume of the natural sand.

Keywords: geopolymer concrete; fine waste glass; RESIN8; metakaolin; slag; mechanical properties

Citation: Ajayi, B.L.; Babafemi, A.J. Effects of Waste Plastic and Glass Aggregates on the Strength Properties of Ambient-Cured One-Part Metakaolin-Based Geopolymer Concrete. *Appl. Sci.* **2024**, *14*, 1856. https://doi.org/10.3390/app14051856

Academic Editor: Syed Minhaj Saleem Kazmi

Received: 13 January 2024
Revised: 16 February 2024
Accepted: 21 February 2024
Published: 23 February 2024

1. Introduction

The construction industry is highly concerned about its contribution to global warming, resulting from the carbon emissions (CO_2) associated with its activities. The primary sources of CO_2 emission in the construction industry are materials production, construction activities, transportation, and waste generation. Portland cement (PC) is one of the major contributors of CO_2 in the industry. This emission emanates from the combustion of carbon-based fuel and the thermal decomposition of limestone in the rotary kiln to produce calcium oxide [1]. The production of 1 kg of PC produces almost an equivalent quantity (0.8–0.9 kg) of CO_2 [2–4]. Additional studies have determined that PC manufacturing accounts for approximately 7% of the worldwide CO_2 emissions [5–7]. Furthermore, an estimated 1.45 ± 0.20 gigatonnes (Gt) of global CO_2 emissions were attributed to cement production in 2016, according to Andrew [8]. This contributed to a cumulative total of 39.3 Gt of CO_2 emissions from 1928 to 2016.

In 1979, Davidovits introduced a novel geopolymer binder produced with calcium- and silicate-rich precursors. Geopolymer binders are formed through a chemical reaction between aluminosilicate materials and alkalis (reagents), resulting in a hardened matrix [9]. This binder is formed by subjecting the precursors to alkalinisation, which

depolymerises the silicates (depolymerisation of silicates) and leads to the gel formation of oligo-sialates. The oligosialates polycondense rearranges to form a network structure and solidify into a hardened geopolymer. This innovative process bypasses the carbon-intensive production of PCs and offers potential environmental benefits. However, the first invented geopolymer binder, known as two-part, is less user and environmentally friendly due to the use of liquid alkali reagents that are corrosive, viscous, and hygroscopic in nature. Consequently, a one-part geopolymer binder was developed, a user- and environmentally-friendly alternative that mitigates the limitations of a two-part geopolymer binder, particularly in mass in-situ concrete production.

Contrary to two-part geopolymer, one-part geopolymer binder requires dry-mixing (similar to conventional binder) of the aluminosilicate precursors with solid reagents before water is then added to promote the dissolution, reorganisation, and polymerisation of the mixture [10]. A one-part geopolymer binder has been found to have a global warming potential that is 22% lower than a two-part geopolymer binder and 65% lower than PC, mainly due to the reduction or substitution of NaOH [7]. Hence, a one-part geopolymer is environmentally friendly compared to a two-part and conventional binder. However, the mix design is challenging and laborious due to the need for exquisite selection and proportion of raw materials, curing method, and the use of effective admixtures to achieve the required workability, setting time, strength, and durability properties. Available studies on one-part geopolymer concrete are mostly focused on fly ash (FA)-based one-part geopolymer binder or concrete, with limited information on metakaolin (MK)-based one-part geopolymer concrete.

MK is a precursor that offers a higher degree of purity in terms of aluminosilicate compared to FA. It is produced by subjecting kaolin to dehydroxylation within a temperature range of 650 °C to 800 °C [11,12]. MK consists of a significant amount, approximately 55% of SiO_2 and Al_2O_3, along with small quantities of other minerals, such as Fe_2O_3 and TiO_2 [13,14]. Still, it lacks calcium oxide, which is the hydration phase of cement. Its primary source (Kaolin) is the most abundant aluminosilicate precursor on earth, with over 5 billion tonnes available [14]. MK is also increasingly recognised and appropriate for engineering applications because of its enhanced durability qualities, which include its resistance to acid attacks and reduction of the effects of efflorescence and alkali-silica reactions (ASR) [15]. Ground granulated corex slag (GGCS) is a molten slag residue obtained from iron steel production through the smelting reduction (corex) process by the ArcelorMittal steel plant in South Africa. This approach is environmentally friendly, unlike the traditional methods involving metallurgical coke and blast furnaces, yielding ground granulated blast furnace slag (GGBS) [16]. The addition of GGCS to MK in the development of a one-part geopolymer binder/concrete is poised to make up for the lack of calcium in MK. The addition of GGCS introduces a binding phase, increases early strength development of the matrix, and allows an ambient curing method.

Using efficient alkali reagents at the optimum proportion is a solution to obtaining sustainable geopolymer concrete. The most used alkali reagents are Na_2SiO_3 and NaOH; however, the exploration of alternative reagents was necessitated by the intensive energy demand of 850–1088 °C in the production of Na_2SiO_3 from the direct fusion of sand and Na_2CO_3 and the generation of CO_2 emissions [7,17,18]. Hence, incorporating $Ca(OH)_2$ reduces dependence on energy-intensive reagents.

$Ca(OH)_2$ has been used as an admixture, which improved the compressive strength of geopolymer binder and led to the early precipitation of calcium silicate hydrate (C-S-H) polymeric gel and enhanced its early age strength development [19,20]. As a result, the presence of $Ca(OH)_2$ encouraged the synthesis of certain products that gave the matrix its stiffness. The use of $Ca(OH)_2$ further increases the calcium content in the geopolymer mixture. It enhances the compatibility of the mixture with the use of admixtures such as superplasticiser and retarder, similar to the conventional PC. Hence, $Na_2SiO_3.5H_2O$, NaOH and $Ca(OH)_2$ were used in this study. However, according to Tan et al. [21], the degree of cement hydration can be indicated by the amount of calcium hydroxide (CH) and

ettringite (AFt), which are common hydration products in cement. The incorporation of calcium-rich precursors in a one-part geopolymer binder leads to the early formation of calcium-containing hydrate, thereby increasing the setting time of the matrix [22]. Prior research has shown that trisodium phosphate is a useful retarding agent in two-part alkali-activated binder (AAB) systems and Portland cement paste [21,23,24]. However, its impact on one-part geopolymer binder or concrete is sparse [17].

In addition, sustainability in the industry is a major challenge due to the excessive consumption of natural resources and the contribution to global waste generation [25,26]. Hence, turning consumable wastes such as waste plastic (RESIN8) and glass into fine grain-size aggregates is beneficial for economical concrete and reduces the environmental pollution caused by these wastes. RESIN8 is a type of recycled waste plastic that encompasses all seven (7) types of plastic. The Centre for Regenerative Design and Collaboration (CRDC) processing operation of RESIN8 involves the collection of these waste plastics from industrial and environmental waste streams, shredding, and subjecting them to melting temperatures ranging from 190 °C to 200 °C for low-density polymers and 230 °C for high-density plastics. The melted plastic is then batched, pre-conditioned to eliminate odours, further melted during the heat extrusion stage, and cooled in water. After drying, the waste plastic is granulated to achieve the desired particle size.

According to estimates by Geyer et al. [27], global plastic production between 1950 and 2015 reached 8800 Mt. Out of this amount, only 2500 Mt (30%) was still in use by 2015, while 600 Mt (9%) was recycled, 800 Mt (12%) was incinerated, and a staggering 4900 Mt (60%) was discarded and found its way into landfills, oceans, and rivers. Their projections for the year 2050 indicate a staggering accumulation of 25 billion metric tonnes of plastic waste. According to Thonecroft et al. [28], up to 15% of fine waste plastic aggregate by volume of sand having similar particle size grading could be used in concrete production. El-Seidy et al. [29] reported that the inclusion of plastic in concrete reduced water absorption, lowered CO_2 emission, improved thermal conductivity, and reduced acid attack [30].

Further, according to the South Africa-State of Waste Report [31], the country consumed approximately 2.753 Mt of glass in 2017, with 71.2% recycled. The remaining 28.8% of waste glass ended up in landfills and the environment, indicating a need for increased glass recycling capacity in South Africa. Previous studies established that the inclusion of fine waste glass in a highly alkaline cementing material increases the alkalinity, resulting in a denser and stronger composite. Subsequently, it led to improved mechanical properties, reduced shrinkage, and water absorption compared to the control sample [32–34]. However, its inclusion in one-part mekakaolin-based geopolymer has not been investigated.

Therefore, this study developed a one-part metakaolin-based geopolymer concrete (OMGPC) mix, investigated the influence of trisodium phosphate on its setting time, and the influence of RESIN8 and fine glass aggregates on the strength and morphological properties of OMGPC.

2. Experimental Details

2.1. Materials

2.1.1. Precursor

The raw materials used to produce the one-part metakaolin-based geopolymer binder (hereafter called OMGPB) included GGCS and MK. The MK used was supplied by Kaolin Group, Western Cape, South Africa. The GGCS was produced by Arcelor Mittal Steel Plant located in Vanderbijlpark and supplied by Pretoria Portland Cement (PPC) Ltd., Pretoria, both in Gauteng, South Africa. The MK is flash calcined with a high pozzolanic reactivity. The XRF analysis shows that MK is predominantly composed of SiO_2 (71.7%) and Al_2O_3 (20.7%), while GGCS is rich in CaO, SiO_2, Al_2O_3, and MgO, as depicted in Table 1. These findings align with previous studies [13,14,16], confirming the consistent chemical composition of MK and GGCS. Further, the percentage sum of SiO_2, Al_2O_3, and

Fe_2O_3 for MK is over 70% recommended by ASTM C618 [35] for pozzolanic materials, hence classifying MK as Class N pozzolan. Further, the basicity modulus (Mb) of GGCS was assessed using Equation (1), which is the ratio of the basic oxides to the acidic oxides present in the slag. The basicity coefficient (K_b) was also evaluated to obtain the suitability of GGCS for concrete application (Equation (2)). The M_b and K_b are 1.06 and 1.93, respectively; hence, the GGCS is a basic slag (since the K_b > 1.1). These results align with the findings of Burciaga-Díaz and Escalante-García [36], supporting the pozzolanic reactivity of GGCS as a beneficial precursor in geopolymerisation processes. In addition, the chemical composition of the recycled aggregate was also determined for a better understanding of their influence on the resultant matrix (Table 1).

$$M_b = \frac{CO + MgO}{SiO_2 + Al_2O_3} \quad (1)$$

$$K_b = \frac{CaO + MgO + Al_2O_3}{SiO_2 + TiO_2} \quad (2)$$

Table 1. Chemical composition of Precursors and recycled aggregates.

Compound	Al_2O_3	CaO	Fe_2O_3	MgO	Na_2O	SiO_2	TiO_2	K_2O	Others
GGCS	14.49	38.24	1.38	11.90	0.18	32.93	0.51	0.55	0.04
MK	20.67	0.04	1.73	0.83	0.36	71.74	0.86	3.12	0.04
RESIN8	3.14	10	0.43	0.35	0.05	7.07	1.42	0.04	0.08
FWG	1.76	10.61	0.62	0.63	12.41	71.92	0.08	0.49	0.13

The specific particle size distribution (PSD) analysis was performed on the precursors using a Mastersizer 2000 instrument and presented in Figure 1. The PSD of MK and GGCS range from 0.02 to 2000 µm with uniformity coefficients of 1.46 and 0.799, respectively, depicting a more uniform distribution of GGCS particles compared to MK (Table 2). The specific gravity of MK and GGCS are 2410 kg/m^3 and 2900 kg/m^3, respectively. The specific surface area of MK is 0.838 m^2/g compared to the GGCS with 0.921 m^2/g, as shown in Table 2, which signifies the higher reactivity of GGCS.

Table 2. Physical properties of precursors.

Precursors	Specific Surface Area m²/g	PSD Range (µm)	D_{50} (µm)	Uniformity Coefficient	Refractive Index
MK	0.838	0.020–2000	12.90	1.46	1.57
GGCS	0.921	0.020–2000	18.78	0.799	1.62

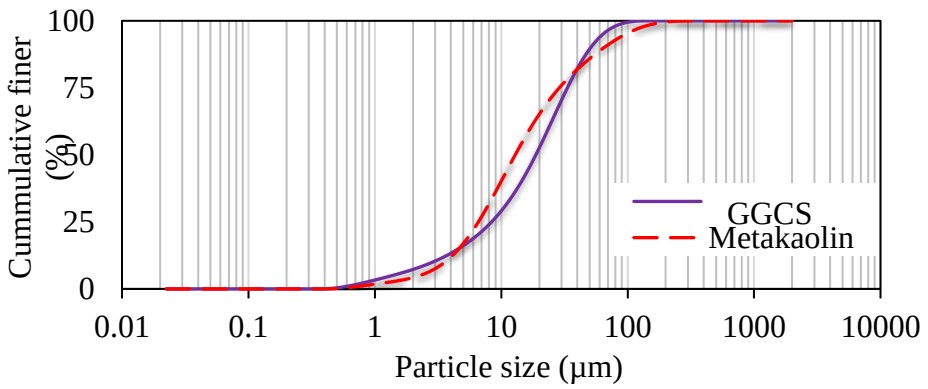

Figure 1. Particle size distribution of precursors.

The scanning electron microscope (SEM) analysis was performed on the precursors using a Zeiss MERLIN (Jena, Germany) instrument available at Central Analytical Facility

(CAF), Stellenbosch University to assess their surface morphology, as presented in Figure 2. The Zeiss MERLIN is an instrument manufactured by Carl Zeiss Microscopy GmbH in Jena, Germany. MK particles are observed to consist of some spherical and non-spherical particles. In contrast, GGCS predominantly consists of mixed-size angular particles, which aids its interlocking and mechanical bonding potential in the OMGPC matrix.

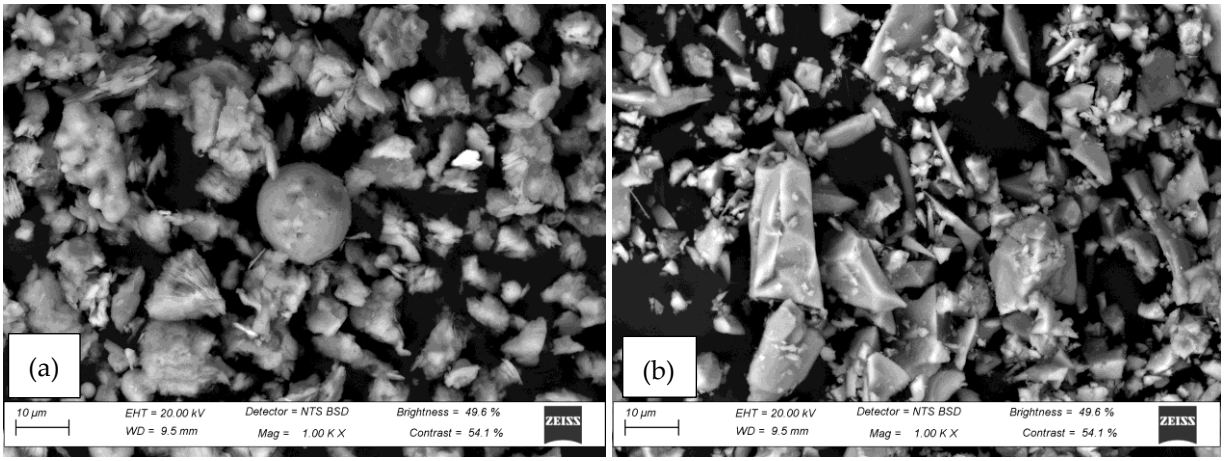

Figure 2. SEM image of precursors (**a**) MK (**b**) GGCS.

2.1.2. Alkali Reagents

The solid alkali reagents used were $Na_2SiO_3.5H_2O$, NaOH, and $Ca(OH)_2$, which were purchased from KIMIX Chemical Lab in Cape Town, South Africa. The $Na_2SiO_3.5H_2O$ (hereafter referred to as SS) comprised 28.56% Na_2O, 27.64% SiO_2, and 43.8% H_2O, with a modulus ratio (SiO_2/Na_2O) of 0.97 and bulk density of 0.86 kg/cm^3. The NaOH (hereafter referred to as SH), which had a 98.8% purity and 0.03% NaCl, was used to adjust the sodium content within the specified range of adoption recommended by Davidovits [17,37,38].

2.1.3. Aggregates

The aggregates used in this study were locally sourced sand (Malmesbury sand), RESIN8, FWG, and a locally sourced coarse aggregate (Greywacke stone). The RESIN8 and FWG were supplied by CRDC and Adargh packaging company, respectively, both in Cape Town, South Africa and presented in Figure 3. The fine aggregates were pre-treated to ensure a similar PSD below 2.36 mm, while the PSD of the coarse aggregate (hereafter referred to as CA) is below 14 m (Figure 4), as obtained through a sieve analysis. The specific gravity (SG) of the RESIN8, FWG, Malmesbury sand, and CA are 1.03, 2.08, 2.67, and 2.72 (Table 3), while the fineness moduli are 2.53, 2.60, 2.34, and 6.75, respectively.

Figure 3. Recycled aggregates (**a**) RESIN8 and (**b**) fine waste glass.

Table 3. Physical properties of aggregates.

Aggregates	SG (kg/m³)	Compacted Bulk Density (kg/m³)	Water Absorption (%)	Moisture Content (%)
Sand	2670	1725	1.42	0.6
RESIN8	1030	445	0.68	0.4
FWG	2080	1387	0.23	0.2
Stone	2720	1580	0.58	0.1

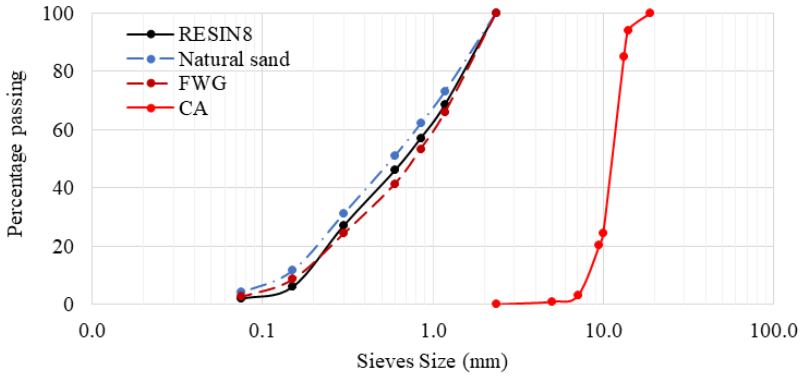

Figure 4. PSD of OMGPC aggregates.

2.1.4. Admixtures and Fibre Reinforcement

The admixtures used were a trisodium phosphate retarder (Na_2PO_4, hereafter referred to as NP), having a molar mass of 163.94 g/mol, and a modified polycarboxylates-based superplasticiser, also known as Chryso Optima 206 SP, purchased from KIMIX Chemical Lab, Cape Town, South Africa. Chryso Optima SP has been investigated in a highly alkaline medium and reported to be effective in enhancing the workability of the mixture [39].

A synthetic fibre known as polyvinyl alcohol fibre (PVA) was used to reduce the shrinkage of the matrix due to the high content of GGCS in the mixture. The PVA was produced by Kuraray CO. Ltd., Chiyoda-ku, Tokyo, Japan. These properties of fibre are shown in Table 4.

Table 4. Properties of PVA fibre.

Fibre	Length (mm)	Diameter (μm)	Young's Modulus (GPa)	Elongation (%)	Specific Gravity (g/cm³)	Tensile Strength (MPa)
PVA	8	40	41	6	1.3	1600

2.2. Methods

2.2.1. OMGPC Mix Design

The mix design was obtained by the packing density method of the aggregates with reference to Raj et al. [40]. The optimum bulk density was obtained by varying the percentage of CA to Malmesbury sand (henceforth called MS) in different proportions at 90:10, 80:20, 75:25, 70:30, 65:35, 60:40, 55:45, and 50:50. The obtained optimum bulk density was used to calculate the packing density for each aggregate proportion. The maximum packing density at a CA:MS of 60:40 was then used for the mix design to obtain the binder, MS, and CA contents in the mix. A Taguchi experimental design approach was adopted to obtain the proportion of the binding materials.

Single-Factor and Orthogonal Experimental Design Using Taguchi Approach

The Taguchi Method is a systematic approach that utilises the Design of Experiment principles to reduce data variability and examine numerous variable parameters with a minimal number of trials. By considering multiple control factors, the method aims to obtain more precise and quantitative results from minimal experiments [41]. Hence, single-factor and orthogonal experiments were designed in accordance with Cimbala [42] and Wang et al. [43]. The single factor mainly includes the percentage proportion of GGCS and MK (A) and the proportion of SS, SH, and CH (B). Experimental formula A: the mixed percentage proportions of GGCS and MK were 70:30, 60:40, and 50:50. However, it was reported by Kuo et al. [44] and Nath and Sarker [45] that more than 60% GGBS will result in higher shrinkage which will reduce the durability of the material. Hence, fibre was incorporated to reduce the shrinkage of the matrix.

Experimental formula B: the mixed percentage proportions of SS, SH, and CH to the binder were 30:40:30, 40:40:20, and 50:30:20. The orthogonal experimental design method was used to determine the effect of each of the designed parameters on the 7-day (7-d) compressive strength (f_c) of OMGPC for optimum design, as depicted in Table 5. There are two parameters (A and B) of the orthogonal experiment, with three levels for each parameter. It is assumed that there is no interaction between the two parameters. The experimental design of the orthogonal arrays consisted of 9 OMGPC mixes designed according to the orthogonal design table $L_3(3^2)$, as shown in Table 6. The setting time of the geopolymer concrete mixture was investigated with 1%, 2%, and 3% contents of the retarder to obtain the efficient content for the mixture and the activator/binder ratio. The efficient retarder/binder ratio was 0.025 (2.5% by wt. of the binder), the water/solid was 0.55 (55%), and the SP to binder ratio was 0.012. 1.5% of PVA by volume of the binder was added to all the trial mixes.

Table 5. Trial mixes and 7-d compressive strength of OMGPC with their oxide molar ratios.

ID	MS (kg/m³)	CA (kg/m³)	Density (kg/m³)	f_c (MPa)	Molar Ratio							
					Na_2O (%)	CaO (%)	Si/Al	Na/Si	Na/Al	(Ca + Mg)O /SiO_2	Ca/Al	Na/Ca
REF1	778	1167	2360	16.33	5.28	29.02	4.38	0.12	0.54	1.06	3.29	0.16
REF2	778	1167	2332	26.34	5.60	28.18	4.41	0.13	0.57	1.03	3.20	0.18
REF3	778	1167	2338	25.60	5.03	28.18	4.45	0.12	0.52	1.02	3.20	0.16
REF4	778	1167	2312	9.94	5.30	25.63	4.50	0.11	0.51	0.87	2.76	0.19
REF 5	778	1167	2334	20.04	5.24	24.78	4.53	0.12	0.55	0.84	2.66	0.20
REF6	778	1167	2313	19.87	4.98	24.78	4.56	0.11	0.48	0.83	2.66	0.18
REF7	778	1167	2244	4.80	5.31	22.24	4.60	0.11	0.49	0.60	2.26	0.22
REF8	778	1167	2265	10.21	5.63	21.39	4.63	0.11	0.52	0.57	2.18	0.24
REF9	778	1167	2296	9.93	5.07	21.39	4.66	0.10	0.47	0.57	2.18	0.21

Table 6. Results and range analysis data of $L_3(3^2)$ orthogonal matrix test.

Factor Number	MK:GGCS (A)	SS:SH:CH (B)	f_c (7-d)
REF1	30:70	30:40:30	16.33
REF2	30:70	40:40:20	26.34
REF3	30:70	50:30:20	25.60
REF4	40:60	30:40:30	9.94
REF 5	40:60	40:40:20	20.04
REF6	40:60	50:30:20	19.87
REF7	05:50	30:40:30	4.80
REF8	50:50	40:40:20	10.21
REF9	50:50	50:30:20	9.93
K_1	22.76	10.36	
K_2	16.62	18.86	
K_3	8.31	18.47	
R	14.45	0.39	

Table 6 shows that K_1 is more efficient in experimental A, while K_2 and K_3 are more efficient in experimental B. Hence, K_1 and K_3 were selected for experimental A and B, respectively. Therefore, the most effective mix design was REF3, which was then used as the control mix for the main study, while other mixes contained RESIN8 and FWG aggregates, respectively, as presented in Table 7.

Table 7. Mix design proportion for OMGPC (all in kg/m^3).

Mark	CA	FA	RESIN8	FWG	MK	GGCS	SS	SH	CH	SP	Fibre	Water
Control	1167	778	0	0	95	265	21.6	12.96	9	4.32	2.55	221.7
R5%	1167	739	15	0	95	265	21.6	12.96	9	4.32	2.55	221.7
R10%	1167	700	30	0	95	265	21.6	12.96	9	4.32	2.55	221.7
G5%	1167	739	0	30.25	95	265	21.6	12.96	9	4.32	2.55	221.7
G10%	1167	700	0	60.53	95	265	21.6	12.96	9	4.32	2.55	221.7

Mix Proportion and Procedure

Table 7 presents the mix proportion of the OMGPC. The MS was substituted with RESIN8 at 5% and 10% by volume of the sand (hereafter referred to as R5% and R10%). In addition, a second batch of the OMGPC was produced with the substitution of MS with FWG at 5% and 10%, hereafter referred to as G5% and G10%. Figure 4 depicts the production chart of the OMGPC, with its mixing process similar to conventional concrete. The OMGPC was mixed in a 50-litre mechanical mixer at a 60 rev/min frequency. The components were dry mixed for 3 min before introducing 60% of the required water, then mixed for another 3 min, and the remaining 40% water mixed with SP was introduced to the mixture. The mixture was further mixed for another 3 min, and the fresh properties of the mixtures were measured. The mixture was then cast into various mould sizes according to the test requirements. The OMGPC matrices were cured in ambient conditions for 7, 28, and 90 days (hereafter referred to as 7-d, 28-d, and 90-d) before various strength properties were investigated, as depicted in Figure 5.

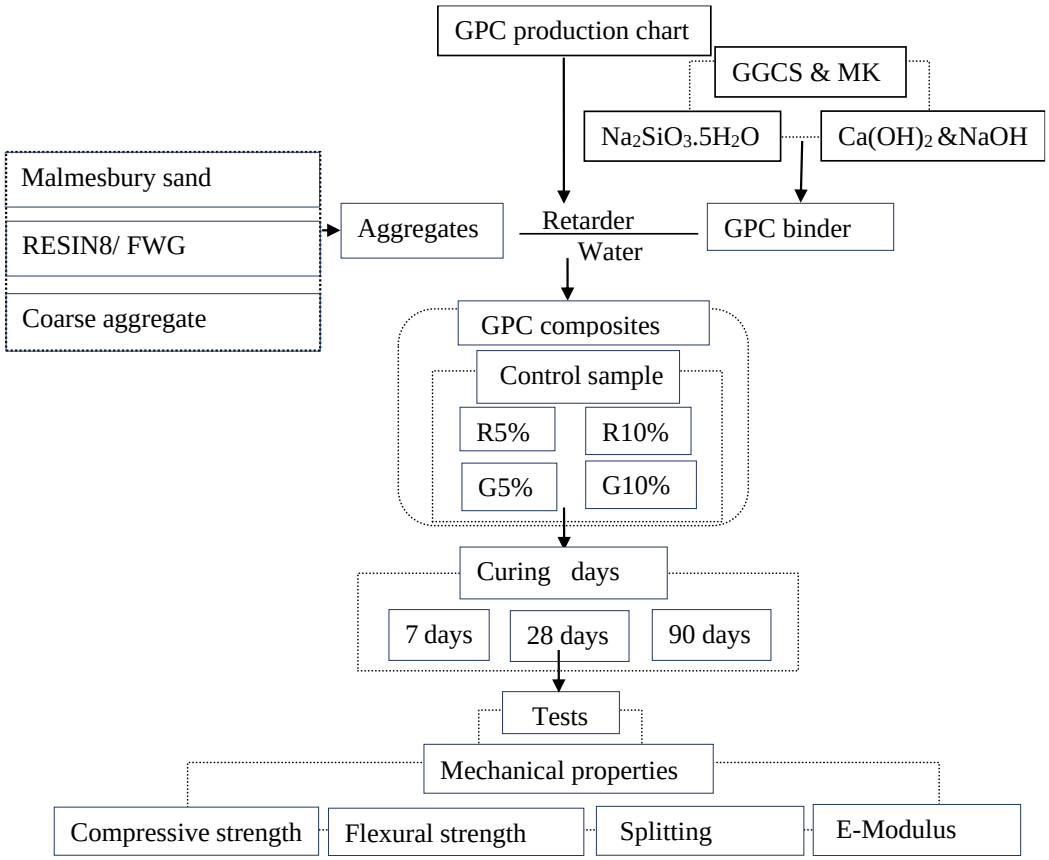

Figure 5. OMGPC programme chart.

2.2.2. Fresh Properties

The investigation of the setting time for the geopolymer binder involved the use of a Vicat apparatus, following the prescribed procedures specified in BS EN 196-3 [46]. To prepare the binder, the constituent materials were batched and thoroughly mixed using a 5-litre mechanical mixer at a revolution of 25 rev/min, ensuring proper homogeneity. The investigation was performed in a climate-controlled room with a constant temperature of 23 °C and 65% relative humidity, providing valuable insights into the behaviour and performance of geopolymer binder during the curing process. The workability of OMGPC was assessed using a slump cone according to procedures outlined in BS EN 12350-2 [47].

2.2.3. Hardened Density and Compressive Strength

The hardened density was determined in accordance with BS EN 12390-7 [48]. A compressive strength test was conducted on 100 mm cube specimens following the specifications of BS EN 12390-7 [48], employing a KingTest Contest machine (manufactured by King Lab Supplies (PTY) Ltd., Johannesburg South Africa) with a loading rate of 180 kN/min until the specimens failed. The failure loads were recorded for each test. The density and compressive strength were calculated based on the average density and strength derived from five cubes per mix, respectively.

2.2.4. Flexural Strength

Three prismatic OMGPC replicates measuring 300 × 100 × 100 mm (length × breadth × width) were cast as per BS EN 12390-1 [49] and BS EN 12390-2 [50]. The specimens were compacted using a vibrating table and cured at an ambient condition. The flexural strength of the specimens was investigated using a four-point bending test on the Zwick Z250 material testing machine (manufactured by Zwick Roell Group, Ulm, Germany) after 7, 28, and 90 days of curing. The load was applied at a constant rate of 0.06 MPa/s until

failure occurred. Hence, the load corresponding to the concrete failure was recorded, and the flexural strength was computed using standard equations as specified in the standard. The flexural strength results were analysed to assess the effect of waste aggregates on OMGPC specimens.

2.2.5. Splitting Tensile Strength

Cylindrical specimens of 100 mm diameter and 200 mm height were used to determine the STS of the OMGPC. Three replicate specimens per mix were subjected to splitting tensile stress of 0.3 MPa/s using a Zwick Z250 material testing machine. . The investigation was performed in adherence to the procedures outlined in BS EN 12390-6 [51].

2.2.6. Modulus of Elasticity

The secant modulus of elasticity test was conducted in accordance with the ASTM C469-02 [52] standard. The testing setup consisted of a Contest testing rig, a Spider8 data logger linked to a computer, three Linear Variable Differential Transducers (LVDTs) placed at 180° from one another, two circumferential rings rigidly attached on the specimen (which bore the LVDTs), and a 2 MN load cell. Cylindrical specimens, measuring 100 mm in diameter and 200 mm in height, were used for the experiment. To determine the individual Young's modulus of elasticity of the 28-d-cured OMGPC, the specimens were subjected to cyclic loading at a level corresponding to 40% of their maximum compressive strength. The specimens were loaded and unloaded, repeated three times, and averaged. A Spider8 data logger was used to record and process the experimental data. Subsequently, the stress-strain relationship and Young's modulus of elasticity were derived from the processed data.

2.2.7. Morphology of OMGPC

The prepared 28-d cured OMGPC specimens with double-sided carbon tape were mounted on aluminium stubs for thin surface gold coating (10 nm thickness) using the Leica EM ACE200 Gold Sputter Coater. This enabled the surface of the specimen to be electrically conductive and avoided electron buildup on the surface, which can result in an electron charge on the scanned image. Subsequently, the specimens were loaded into a Zeiss MERLIN Field Emission Scanning Electron Microscope, an instrument manufactured by Carl Zeiss Microscopy GmbH in Jena, Germany. SmartSEM 5 software, Oxford and AZTEC (v.6.1.) (Energy system software, Oxford instrument) were utilised to investigate the morphological information of the specimens through in-lens electron images. Inlens electron SEM collects the secondary electrons (SE2), which were generated by direct interaction with the incident electron beam. The imaging was carried out at a magnification of 10–20 KV for better resolution and quality images. This test is relevant to evaluate the heterogeneity, the ITZ, and morphology of the mixes.

3. Results and Discussion

3.1. Fresh Properties and Density of OMGPC

3.1.1. Setting Time of One-Part Metakaolin-Based Geopolymer Binder

The control geopolymer binder exhibits a final setting time below 2 h with an initial setting time below 1 h, confirming the rapid setting nature of the material. However, the inclusion of Na_3PO_4) has proven effective in retarding the setting rate of the geopolymer mixture. By incorporating 3% Na_3PO_4, the initial and final setting time are extended by an additional 1 h:52 min (238.3%) and 2 h:30 min (133.9%), respectively, compared to the control, as depicted in Figure 6 The use of 2–3% of Na_3PO_4 is suitable for retarding the setting time of an OMGPC, which gives an open time of 3–4 h for geopolymer concrete production. This finding is consistent with a similar report by Gong and Yang [53], which supports using Na_3PO_4 as a setting retarder in geopolymer binder.

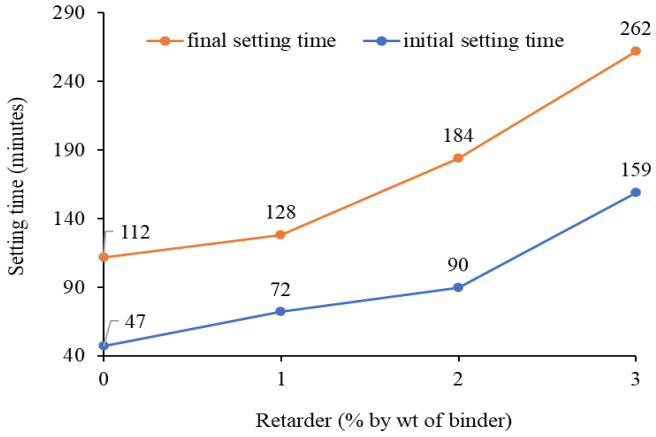

Figure 6. Influence of Na_3PO_4 on setting time of geopolymer binder.

3.1.2. Workability of OMGPC

Figure 7 shows that incorporating R5% and R10% improves the workability by 5.6% and 13.7%, respectively, while G5% and G10% enhanced the workability of OMGPC by 15.8% and 26.3%, respectively, compared to the control mix. The improved workability of the OMGPC incorporating RESIN8 is attributed to the hydrophobic nature of plastic. However, the OMGPC mixes with FWG aggregates possess higher workability than specimens with RESIN8 aggregate. This improved workability of concrete containing FWG over plastic-containing mixtures is also reported in a study performed by Steyn et al. [34]. Further, enhanced workability in concrete containing FWG aligns with the previous findings [54–57]. As obtained from the physical characterisation of aggregates, the water absorption of sand, RESIN8, and FWG are 1.42%, 0.63%, and 0.23%, respectively, hence contributing to the improved workability of the FWG-contained OMGPC mixtures compared to others. In addition to the lower water absorption property of FWG aggregate compared to RESIN8 and sand, Wu et al. [57] noted that the improved workability is attributed to the smooth surface of the FWG aggregate, allowing free water flow in the mixture. Hence, substituting natural sand with these recycled aggregates would reduce the water demand for concrete production.

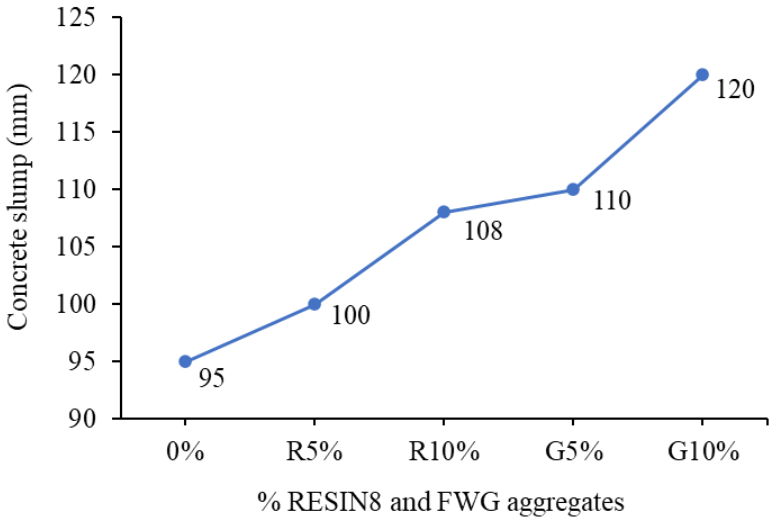

Figure 7. Workability of OMGPC containing RESIN8 and FWG.

3.1.3. Fresh Density of OMGPC

The inclusion of recycled aggregates influences the fresh density of OMGPC, as depicted in Figure 8. An increase in the percentage of RESIN8 content led to a progressive decrease in the fresh density of OMGPC, with a 1.8% reduction for R5% and a 3.7% reduction for R10%, compared to the control specimen. At the same time, there is a minimal decrease in the fresh density of OMGPC containing FWG. The fresh density of G5% and G10% was reduced by 1% and 0.9%, respectively. The reduction in the fresh density of OMGPC containing recycled aggregates is attributed to the lightweight property of RESIN8 and FWG, which is evident from the SG and bulk density obtained from the physical characterisation of the aggregates. The SG of MS is 64% and 22% higher than RESIN8 and FWG, respectively. Meanwhile, the bulk density of MS is 74% higher than RESIN8 and 20% higher than FWG. Adamu et al. [58] and Haruna et al. [59] attributed the reduction in the weight of the matrix containing plastic aggregate to the hydrophobic nature of plastic, which traps air between itself and other aggregates in the matrix.

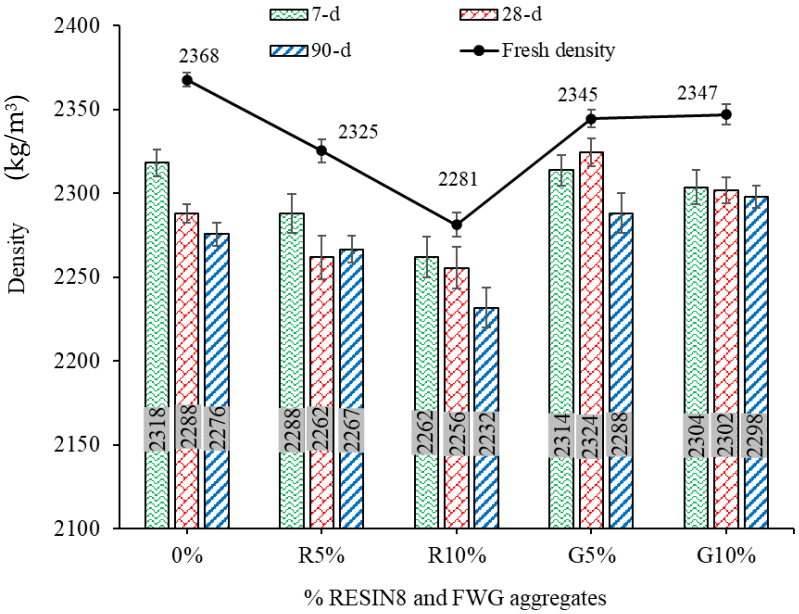

Figure 8. The fresh and hardened density of OMGPC containing recycled aggregates.

3.2. Hardened Properties of OMGPC

3.2.1. Hardened Density of OMGPC

Figure 8 presents the hardened density of OMPGC incorporating RESIN8 and FWG. The inclusion and increase in the content of RESIN8 lead to a decrease in the hardened density of OMGPC at increasing curing age. The reduction in hardened density is attributed to the lightweight properties of RESIN8, which are evident from the SG and bulk density, as presented in Section 3.1.3. Previous studies have established that the density reduction of concrete containing recycled waste plastic depends on the percentage substitution contents [60–63]. The hardened density of OMGPC decreased by 1.1% and 1.4% after 28d of ambient curing for R5% and R10% specimens, respectively, compared to the control specimen. The percentage reduction in the fresh density of the R5% specimen is similar to the percentage reduction in its hardened density.

In contrast, the percentage reduction in the fresh density of the R10% specimen is higher than its hardened density. This could be attributed to the higher porosity of the OMGPC containing RESIN8 in its fresh state, in addition to the lightweight properties of RESIN8. However, the hardened density of OMGPC-containing RESIN8 ranges from 2232 to 2318 kg/m^3, classifying them as normal-weight concretes. In contrast to RESIN8

containing OMGPC, substituting MS with FWG results in an improved hardened density, which aligns with the previous investigation performed on these aggregates by Hajimohammadi et al. [64] and Tayeh et al. [65]. The hardened density (at the 28-d) of G5% and G10% increased by 1.6% and 0.6%, respectively, compared to their control specimens. The hardened density of OMGPC containing FWG ranges from 2288 to 2324 kg/m^3 (normal-weight concrete), as depicted in Figure 8.

3.2.2. Compressive Strength of OMGPC

Figure 9 illustrates the compressive strength characteristic of OMGPC, investigating the influence of RESIN8 and FWG aggregates at various percentage contents. The compressive strength of OMGPC containing RESIN8 decreases as the RESIN8 increases; however, the strength increases with curing age. There is an increase in the compressive strength of OMGPC with increasing FWG and curing age. The compressive strength of the control specimen cured at 28 days is 28.6 MPa, while the strength decreased by 15.7% and 24.1% for R5% and R10%, respectively. The decrease in the OMGPC containing RESIN8 is attributed to the lower stiffness and SG of plastic, the high porosity, and the weak interfacial transition zone (ITZ) between the RESIN8 aggregate and the matrix, which is less stiff compared to the ITZ between natural sand and FWG aggregate-containing GPC [28,63,66–68]. El-Seidy et al. [69] reported that the hydrophobic nature and smooth surface of RESIN8 induce weak interfacial bonding between the RSINE8 and other aggregates, leading to strength reduction of OMGPC. In addition, the high compressibility or deformability of RESIN8 results in more cracks around the aggregate when subjected to compression, hence the reason for strength decrease with the inclusion of RESIN8 [59,70]. An increase in RESIN8 content in OMGPC increases the porosity and reduces the weight of the matrix, thereby resulting in strength reduction.

The strength of OMGPC containing G5% increases by 3.5%, and the OMGPC containing G10% has a similar compressive strength to the control. Steyn et al. [34] also reported an enhanced concrete strength with the substitution of sand with FWG aggregate and strength reduction when substituted with recycled waste plastic aggregate in conventional concrete. This phenomenon can be attributed to the higher stiffness of FWG particles compared to RESIN8 and the participation of silicate oxide from the FWG aggregate in the polymerisation reaction, which further elevates the SiO_2/Al_2O_3 ratio of the mixture. The presence of FWG aggregates also enhances the alkalinity of the matrix, promoting greater reactivity and dissolution around the aggregates. It was reported by Hajimohammadi et al. [32] that as the geopolymer growth progresses, the amorphous FWG content actively participates in the reaction, resulting in a robust, stronger, and compact matrix formation. This explains the reason for the improved strength of OMGPC with FWG aggregate. The additional silicate supplied by FWG further reacts with the $Ca(OH)_2$ reagent to produce more C-S-H gel, which results in a compressive strength increment of the OMGPC [71]. According to the XRD analysis performed, the C-S-H gel increases with an increase of up to 20% of FWG in the matrix [71]. The polymerisation reaction of SiO_2 in FWG with alkaline reagent $Ca(OH)_2$ improves the compactness and the microscopic pore structure within the matrix [72]. Gholampour et al. [33] and Wu et al. [57] obtained GPC with an improved compressive strength at the full substitution of sand with FWG compared to the control, signifying the participation of the chemical composition of FWG in the polymerisation reaction. Hence, the reason for the increased strength is the inclusion of FWG in OMGPC. However, their report revealed that incorporating about 25% of FWG in GPC can decrease strength due to the weakened ITZ between the FWG aggregate and the sand. Hence, the ITZ weakens as the FWG content increases from G5% to G10%, leading to a slight strength reduction at G10% inclusion. This phenomenon explains the incompatibility of the ITZ of natural sand and FWG due to the smooth surface of the glass aggregates. However, their result shows that the ITZ can be improved by incorporating a high quantity of FWG (about 50% above) in GPC. The improved ITZ is evident at the full substitution of sand with FWG by Gholampour et al. [33], leading to enhanced strength.

Further, more FWG aggregate would increase the SiO_2/Al_2O_3 ratio over other oxide ratios due to more SiO_2 supplied by higher percentage contents (10%) of FWG. An increase in FWG in the OMGPC mixture could result in a chemical composition imbalance and reduce the strength of the resultant. According to Davidovit [37,38], the molar ratios of the reactant influence the stability and strength development of GPB or GPC.

In addition, after the 7d of curing, the rate of strength development in OMGPC is relatively minimal, as 98% of the 28-d strength is already attained (Figure 9). For the control specimen, the strength increase between the 7-d and 28-d of curing is 6.7% and 1% increase from the 28-d to 90-d. These results align with findings in previous studies, supporting the assertion that geopolymer binder/concrete exhibits early-age strength development and does not necessitate temperature curing [73–76].

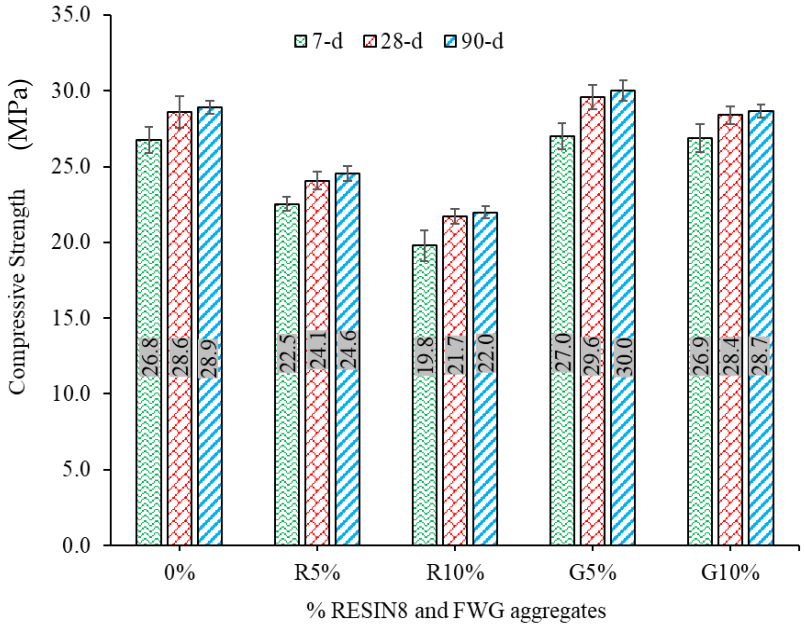

Figure 9. Compressive strength of OMGPC containing RESIN8 and FWG.

3.2.3. Flexural Strength of OMGPC Containing Recycled Aggregates

The flexural strength investigation of OMGPC is necessary to assess its ability to withstand deformation when subjected to bending stress. The flexural strength follows a similar trend to the compressive strength, as depicted in Figure 10. The strength decreases as the content of RESIN8 increases, showing the effect of higher porosity, lower stiffness, and weak ITZ between the RESIN8 aggregate and the natural aggregate. The flexural strength of OMGPC obtained in this study after the 28-d of curing ranges from 3.07 to 4.47 MPa (Figure 10).

The flexural strength of the control OMGPC specimens increases with curing age from 3.25 to 4.17 MPa at the 7-d to 90-d of curing. In addition, the flexural strength of OMGPC increases progressively with curing age for all replacement levels. For OMGPC with RESIN8, the flexural strength decreased as the RESIN8 content increased. However, the difference in flexural strength between the control specimen and the R5% specimen is minimal. Specifically, the R5% specimen has a 9.6% and 5.5% reduction in flexural strength for the 28-d and 90-d cured specimens, respectively, compared to the control.

Meanwhile, the R10% specimen yielded a more substantial decrease, with a 24.6% and 22.1% reduction in flexural strength at the 28-d and 90-d of curing, respectively. This reduction is attributed to the lower stiffness and higher porosity of the RESIN8 aggregate. This flexural strength reduction of concrete incorporating RESIN8 is attributed to lower stiffness and weak ITZ between the surface of the recycled plastic aggregate and the

cement matrix due to the hydrophobic nature of the aggregates, which creates a wall impact and low stiffness compared to sand, as reported by many authors [63,68,77,78].

In contrast, incorporating G5% in OMGPC mixture leads to similar flexural strength of the control specimen at the 28-d of curing, while the strength improves after the 90-d of curing. However, adding G10% leads to an 8.6% and 3.8% flexural strength reduction at the 28-d and 90-d of curing, respectively. Furthermore, the flexural strength is 14.2%, 15.3%, 14.1%, 13.7%, and 13.1% for 0%, R5%, R10%, G5%, and G10% replacement levels, respectively, in comparison to their respective compressive strengths at the 28-d of curing.

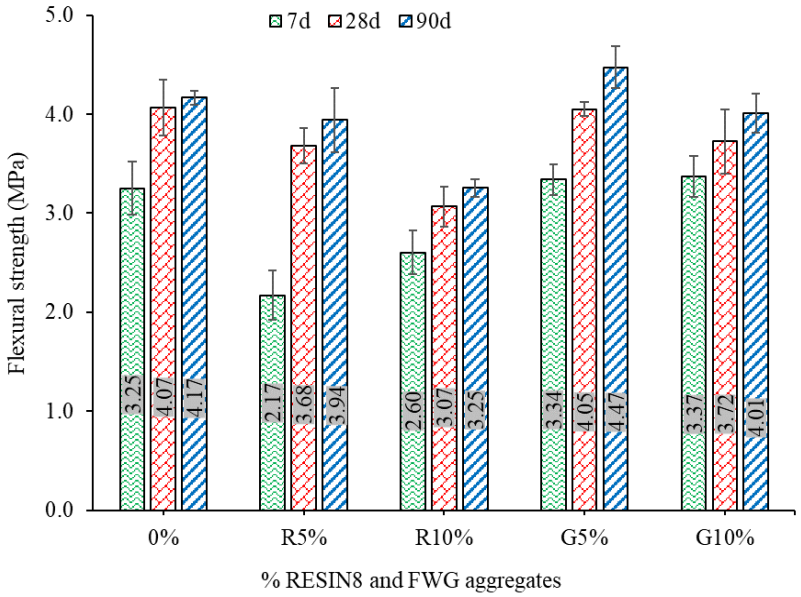

Figure 10. Flexural strength of OMGPC containing RESIN8 and FWG.

3.2.4. Splitting Tensile Strength

The result of the splitting tensile strength (STS) of OMGPC containing recycled aggregates is shown in Figure 11. The control specimen exhibits a maximum STS of 2.7 MPa and 2.8 MPa at the 28-d and 90-d of curing, respectively. The STS values decrease with the addition of RESIN8, with an insignificant increase observed with curing age. Notably, at the 7-d of curing, the control specimen of OMGPC achieved 98% of its 28-d STS. The failure pattern of STS specimens is shown in Figure 12.

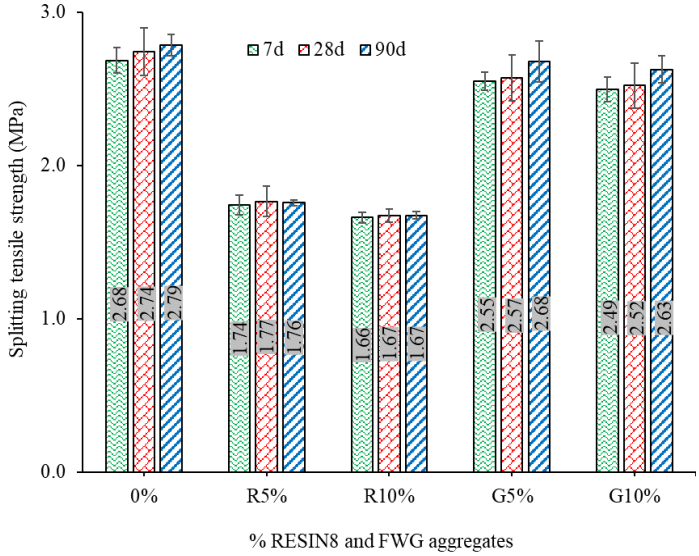

Figure 11. Splitting tensile strength of OMGPC containing RESIN8 and FWG.

Figure 12. Failure pattern of STS specimens.

Compared to the control specimen, incorporating R5% aggregate reduces the STS substantially, with a 34.4% and 36.9% decrease at the 28-d and 90-d of curing, respectively. Similarly, the inclusion of R10% content resulted in a significant STS reduction, with 39.1% and 40.1% reductions at the 28-d and 90-d of curing, respectively.

These reductions are ascribed to the lower stiffness, weak ITZ around plastic aggregate, and higher porosity of the plastic aggregate in the concrete mix. However, compared to the compressive strength of OMGPC reported in Figure 9, the STS of OMGPC at the 28-d is relatively lower. The STS values are 9.6%, 7.3%, 7.7%, 8.7%, and 8.9% of their respective compressive strengths for 0%, R5%, R10%, G5%, and G10% specimens. However, according to Gagg [79], the splitting tensile strength of concrete is often around 8–14% of the compressive strength. Hence, the STS of the OMGPC incorporating RESIN8 is below the range.

In contrast, the STS values of OMGPC with FWG aggregates were similar to the control specimens. The inclusion of FWG aggregate did not lead to significant changes in the concrete's STS. Notably, the STS of the control specimen was well preserved, and the FWG aggregate demonstrated compatibility with the concrete mix. The inclusion of FWG aggregates did not significantly impact the STS, indicating its potential as an alternative and compatible aggregate material for OMGPC application. This report agrees with the findings of Malik et al. [55], showing that the inclusion of FWG up to 10% has no significant difference compared to the control specimen. However, Wu et al. [57] reported that adding 25% of FWG in FA-based geopolymer concrete resulted in a decrease in the STS, but an increase in the FWG from 25% to 75% improved the STS of the composite. Hence, they attributed the improvement of STS to the participation of FWG in the polymerisation reaction.

3.2.5. Static Modulus of Elasticity of OMGPC Incorporating Recycled Aggregates

Figure 13 presents Young's modulus of elasticity of OMGPC with RESIN8 and FWG aggregates. Adding these aggregates resulted in a significant reduction in the elastic modulus compared to the control OMGPC. The control OMGPC exhibited an elastic modulus of 33 GPa. However, incorporating R5% leads to a substantial 60% reduction in the matrix stiffness against deformation. At the incorporation of R10% in OMGPC, the elastic modulus experienced an even more drastic reduction of 78.8%. These findings indicate that the inclusion of RESIN8 aggregates above 5% significantly weakens the overall stiffness and rigidity of the OMGPC matrix. This result is consistent with the previous studies on the use of recycled waste plastic in concrete production, ascertaining that the increase in the recycled aggregate content results in a decrease in the elastic modulus of the concrete [80,81].

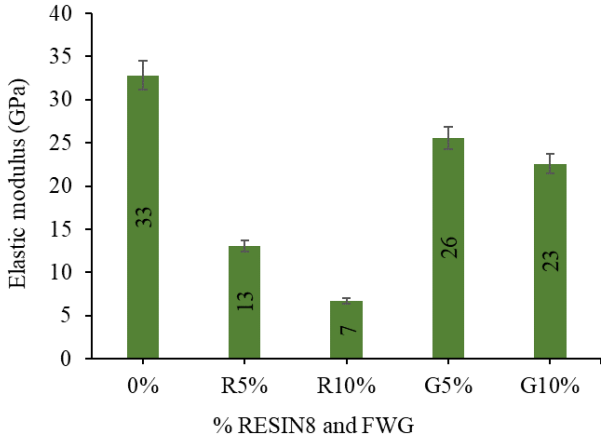

Figure 13. Elastic modulus of OMGPC.

Similarly, adding FWG aggregates also has a notable impact on the elastic modulus of OMGPC. With a G5% content, the elastic modulus decreased by 21.2%, while a G10% content resulted in a more significant reduction of 30.3%. Wu et al. [57] reported a decrease in Young's modulus of elasticity of OMGPC with the inclusion of FWG, which was attributed to the weak glass-geopolymer interfaces. The observed reductions in elastic modulus for both plastic and FWG aggregates are important considerations for structural applications that rely on the stiffness of the concrete and the ability to withstand deformation under loads. The lower elastic modulus may affect the overall behaviour and performance of OMGPC elements, especially in cases where stiffness and resistance to deformation are critical design factors.

3.3. Comparison between Strength Properties of OMGPC

The relationship between compressive and tensile or flexural strength is only empirical since the elements that affect tensile or flexural strength and compressive strength, such as paste content, aggregate type, temperature fluctuations, and shrinkage stresses, differ slightly [82]. The interrelationship between the mechanical properties of OMGPC is necessary to understand its performance and formulation to meet specific application requirements and strength projections.

The power regression model was used for OMGPC containing RESIN8 and FWG. The power regression model generates a good fit for OMGPC containing RESIN8. In contrast, it is not a good prediction model for FWG-containing OMGPC, and a polynomial regression model could not be used due to the limited three data points, which will generally lead to an R^2 of 1. However, for more accuracy using the polynomial regression model for OMGPC containing FWG, more data points would be beneficial compared to the three data points used in this study.

3.3.1. Relationship between Compressive Strength and Hardened Unit Weight

Figure 14 presents the relationship between the compressive and hardened unit weight of 28-d cured OMGPC containing recycled aggregates. The correlation coefficient (R^2) for the concrete containing RESIN8 is 0.9651, and FWG is 0.7104 (Figure 14). Hence, the power equation presented in Equations (3) and (4) gives a 96.5% and 71% prediction of the hardened unit weight of OMGPC incorporating RESIN8 and FWG, respectively, from the compressive strength. Hence, there is a good relationship between these two hardened properties, and a decrease in the hardened density affects the compressive strength of OMGPC incorporating RESIN8 and FWG.

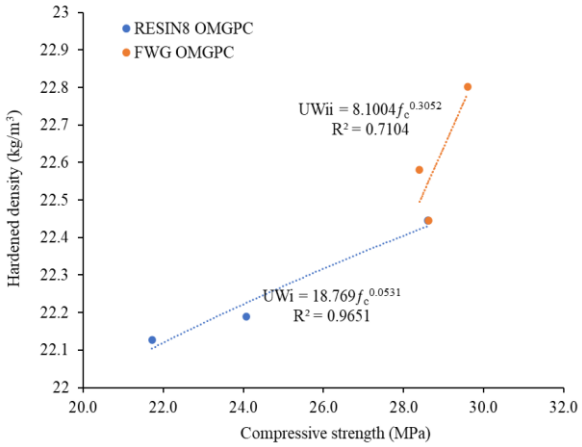

Figure 14. Relationship between the f_c and the hardened unit weight of OMGPC containing RESIN8 and FWG.

$$UW_i = 18.7697 f_c^{0.0531} \quad (3)$$

$$UW_{ii} = 8.1004 f_c^{0.3052} \quad (4)$$

where UW_i is the Unit weight (kN/m³) and f_c = compressive strength (MPa).

3.3.2. Relation between Compressive, Flexural, and Splitting Tensile Strengths

The relationship between the compressive, flexural and splitting tensile strength of OMGPC containing RESIN8 is presented in Figure 15. The relationship between the two strengths of conventional concrete was established in ACI committee 318 [83] and Eurocode EN 1992 [84], as depicted in Equations (5) and (6), respectively. Almeshal et al. [68] obtained a relationship between the compressive and flexural strengths of convectional concrete containing waste plastic aggregate from the data gathered from various studies performed by different authors, as shown in Equation (7).

$$f_f = 0.62\lambda f_c^{0.5} \quad (5)$$

$$f_f = 0.30 f_c^{0.667} \quad (6)$$

$$f_t = 0.09 f_c^{0.97} \quad (7)$$

where λ = is a modification factor, λ for normal and lightweight concrete = 1, and f_f = flexural strength (MPa).

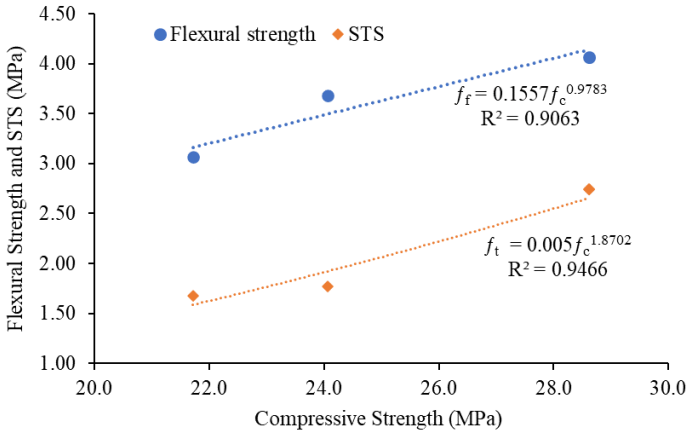

Figure 15. Relationship between f_c and $f_f$of OMGPC containing RESIN8.

The compressive and flexural strength relationship of the OMGPC containing RESIN8 obtained in this study is presented in Figure 15 and Equation (8). The correlation coefficient (R^2) for OMGPC containing RESIN8 is 0.9063, which indicates a good alignment between the model and data, with the closest R^2 to 1 symbolising good correlation. Equation (9) presents the relationship between the compressive and STS of OMGPC containing RESIN8 with an R^2 of 0.9466, as depicted in Figure 15. In contrast, the power model equation for predicting the flexural and compressive strength relationship of OMGPC containing FWG has an R^2 of 0.3759, which is not a good fit for strength prediction; hence, the graph is not presented in this study.

$$f_f = 0.1557 f_c^{0.9783} \quad (8)$$

$$f_t = 0.005 f_c^{1.8702} \quad (9)$$

Figure 16 presents the relationship between the compressive and flexural strength of OMGPC and previous studies on concrete incorporating fine waste plastic [85,86]. The power model equation is depicted in the figure. However, there is variation in the strength predictive equations obtained by various authors, re-establishing that the elements that affect strength properties are slightly different. Further, the relationship between the compressive strength and STS of OMGPC incorporating RESIN8 and some of the previous studies on convectional concrete incorporating fine waste plastic is presented in Figure 17 [82,87].

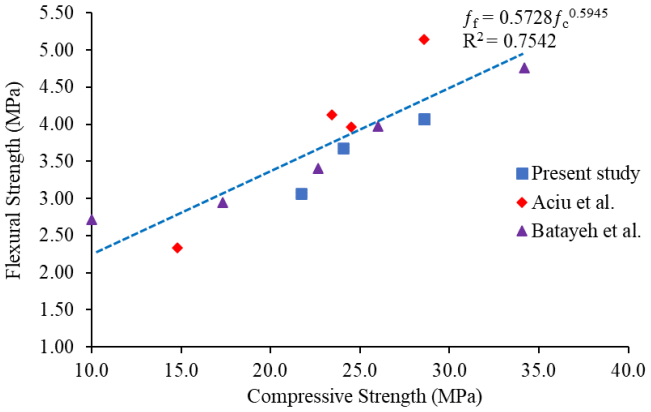

Figure 16. Relationship between the f_c and f_f of OMGPC containing RESIN8 and previous studies on concrete containing fine waste plastic (◆ Aciu et al. [86], ▲ Batayeh et al. [85])

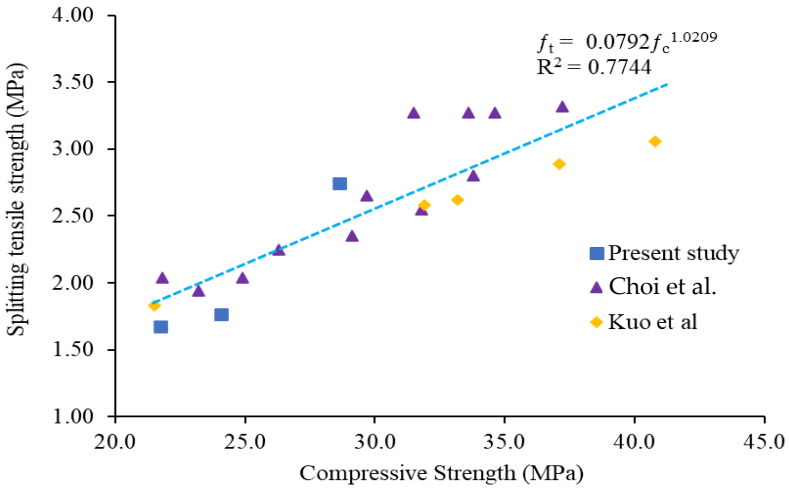

Figure 17. Relationship between compressive and f_f of OMGPC with RESIN8 and previous studies on waste plastic aggregate. (▲ Choi et al. [82], ◆ Kuo et al. [87])

3.4. Morphology of One-Part Metakaolin-Based Geopolymer with Recycled Aggregates

Figure 18 presents the SEM images of OMGPC containing different contents of RESIN8 and FWG. The SEM image of 0% OMGPC (control specimen) shows fewer microcracks and less weak ITZ compared to specimens with recycled aggregates. The addition of R5% content in the mix generates weak ITZ within the matrix, consequently leading to more microcracks in the OMGPC. Furthermore, the inclusion of R10% content in OMGPC results in a higher porosity of the matrix, characterised by a honeycomb-like structure, as depicted in Figure 18 (R10%).

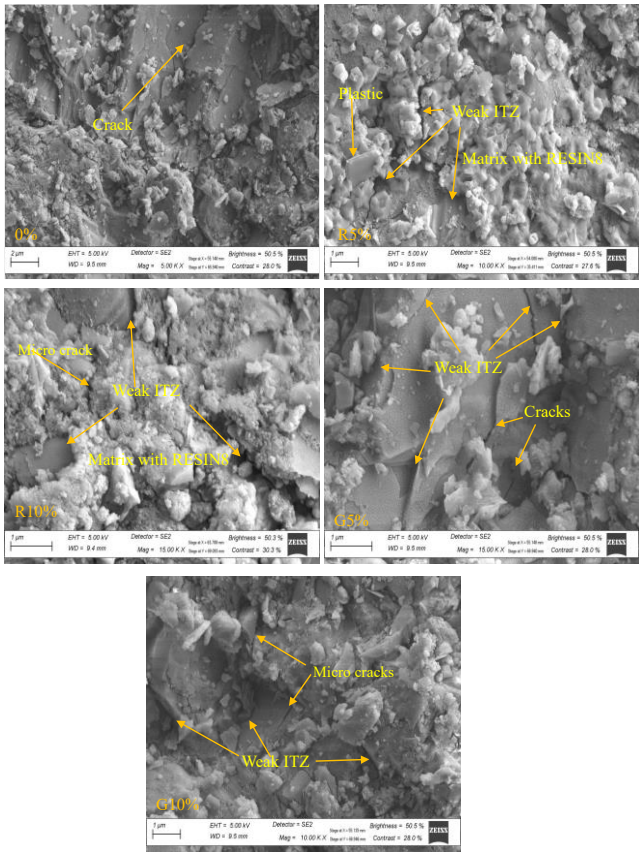

Figure 18. SEM images of OMGPC containing RESIN8 and FWG.

The higher porosity, the weaker ITZ and the lower stiffness of the RESIN8 aggregate contribute to the reduced strength of OMGPC containing RESIN8 contents. Further, there is a reaction between the geopolymer gel and the RESIN8, as depicted on the RESIN8-containing OMGPC (Figure 18). Choi et al. [82] reported that the geopolymer binder adhered to the surface of the waste plastic aggregate reacts with CaOH made by C_2S and C_3S and produces C-S-H. Adding FWG leads to an improved and condensed OMGPC morphology and enhanced geopolymerisation reactions in the matrix. However, at G10% inclusion, the geopolymer structure becomes weakened or loosed due to a weak ITZ and a frictionless surface of the FWG aggregate (G10% specimen). These morphological observations explain the mechanical performance variations in the OMGPC specimen with the inclusion of different FWG content.

4. Conclusions

This study investigated the performance of one-part MK-based geopolymer concrete and the effects of RESIN8 and FWG as partial replacements of natural sand (5% and 10% by volume) on its properties. The following conclusions are drawn from the investigation:

1. The inclusion of R5%, R10%, G5%, and G10% improved the workability of OMGPC by 5.3%, 13.7%, 15.8%, and 26.3%, respectively. However, replacing natural sand with RESIN8 reduced the fresh density of OMGPC; on the other hand, the addition of FWG led to improved fresh density. In addition, 2–3% trisodium phosphate by wt. of the binder effectively retard the early setting time of OMGPB by 238.3% (initial setting time) and 133.9% (final setting time) compared to the control.
2. The hardened density of OMGPC at all replacements for RESIN8 and FWG ranges from 2232 to 2324 kg/m^3, classifying them as normal-weight concrete. However, the inclusion of R5% and R10% reduced the hardened density by 1.1% and 1.4%, respectively, while G5% and G10% improved the density by 1.6% and 0.6%, respectively, for 28 days of cured specimens.
3. A 28.6 MPa OMGPC (at 28 days curing) is obtained in this study, which could be used for structural concrete. The inclusion of R5% and R10% decreased the 28-day strength by 15.7% and 24.1%, respectively. While G5% improved the 28-day strength by 3.5%, and G10% had similar strength to the control.
4. The flexural and splitting tensile strengths decreased with an increase in RESIN8 but increased with the inclusion of FWG.
5. The Young's modulus of elasticity of OMGPC was drastically reduced with the incorporation of RESIN8 and FWG. The addition of R5% and R10% decreased the Young's modulus by 60.6% and 78.8%, respectively, while G5% and G10% contents in OMGPC led to 9.1% and 30.3% decrease in the Young's modulus of the matrices, respectively.
6. The RESIN8 and FWG induced porous structure and weak ITZ in the concrete matrix.

It is recommended that the incorporation of RESIN8 as a substitute for sand in OMGPC be optimised. This should focus on developing strategies to reduce the porosity induced by plastic and improving the ITZ between the plastic aggregates and OMGPC. In addition, the durability properties of OMGPC should be investigated to better understand its resistance to environmental factors, such as freeze-thaw cycles, chemical exposure, and long-term exposure to moisture.

Author Contributions: Conceptualization, B.L.A. and A.J.B.; methodology, B.L.A.; validation, B.L.A.; formal analysis, B.L.A.; investigation, B.L.A.; resources, A.J.B.; data curation, B.L.A.; writing—original draft preparation, B.L.A.; writing—review and editing, A.J.B.; visualisation, B.L.A.; supervision, A.J.B.; project administration, A.J.B.; funding acquisition, A.J.B. All authors have read and agreed to the published version of the manuscript.

Funding: This research received no external funding.

Institutional Review Board Statement: Not applicable.

Informed Consent Statement: Not applicable.

Data Availability Statement: The raw data supporting the conclusions of this article will be made available by the authors on request. The data are not publicly available due to privacy.

Acknowledgments: The authors are grateful to the Postgraduate Scholarship Programme Committee, Stellenbosch University, South Africa. The authors' appreciation also goes to the Kaolin Group (Pty) Ltd., CRDC, and Adargh packaging Company, all in Cape Town, South Africa, for donating Metakaolin (MK_{60}), RESIN8, and fine waste glass, respectively, for this study. Kehinde Awokoya of the Chemistry Department, Obafemi Awolowo University, Nigeria, is also appreciated for his valuable comments during the preparation of this manuscript.

Conflicts of Interest: The authors declare no conflicts of interest.

References

1. Chen, I.A.; Juenger, C.G. Incorporation of waste materials into Portland cement clinker synthesised from reagent-grade chemicals. *Int. J. Appl. Ceram. Technol.* **2009**, *6*, 270–278.
2. Huntzinger, D.N.; Eatmon, T.D. A life-cycle assessment of Portland cement manufacturing: Comparing the traditional process with alternative technologies. *J. Clean. Prod.* **2009**, *17*, 668–675.
3. Davidovits, J. Global Warming Impact on the Cement and Aggregates Industries. *World Resour. Rev.* **1994**, *6*, 263–278.
4. Adesina, A. Performance and sustainability overview of sodium carbonate activated slag materials cured at ambient temperature. Resources *World Resour. Rev.* **1994**, *6*, 263–278.
5. International Energy Agency. Cement Technology Roadmap Plots Path to Cutting CO_2 Emissions 24% by 2050. Available online: https://www.iea.org/news/cement-technology-roadmap-plots-path-to-cutting-co2-emissions-24-by-2050 (accessed on 12 September 2023).
6. Wan-En, O.; Yun-Ming, L.; Cheng-yong, H.; Ngee, H.L.; Abdullah, M.M.A.B.; Khalid, M.S.B.; Loong, F.K.; Shee-Ween, O.; Seng, T.P.; Jie, H.Y.; et al. Towards greener one-part geopolymers through solid sodium activators modification. *J. Clean. Prod.* **2022**, *378*, 134370.
7. Neupane, K. Evaluation of environmental sustainability of one-part geopolymer binder concrete. *Clean. Mater.* **2022**, *6*, 100138.
8. Andrew, R.M. Global CO_2 emissions from cement production. *Earth Syst. Sci. Data* **2018**, *10*, 195–217.
9. Palomo, A.; Grutzeck, M.W.; Blanco-Varela, M.T.; Palomo, A.; Blanco, M.T. Alkali-Activated Fly Ashes-A Cement for the Future Alkali-activated fly ashes A cement for the future. *Cem. Concr. Res.* **1999**, *29*, 1323–1329.
10. Duxson, P.; Fernández-Jiménez, A.; Provis, J.L.; Lukey, G.C.; Palomo, A.; van Deventer, J.S. Geopolymer technology: The current state of the art. *J. Mater. Sci.* **2007**, *42*, 2917–2933.
11. Cong, P.; Cheng, Y. Advances in geopolymer materials: A comprehensive review. *J. Traff Transp. Eng.* **2021**, *8*, 283–314.
12. Long, W.J.; Lin, C.; Tao, J.L.; Ye, T.H.; Fang, Y. Printability and particle packing of 3D-printable limestone calcined clay cement composites. *Constr. Build. Mater.* **2021**, *282*, 122647.
13. Bignozzi, M.C.; Manzi, S.; Lancellotti, I.; Kamseu, E.; Barbieri, L.; Leonelli, C. Mix-design and characterisation of alkali activated materials based on metakaolin and ladle slag. *Appl. Clay Sci.* **2013**, *73*, 78–85, 2013.
14. Elzeadani, M.; Bompa, D.V.; Elghazouli, A.Y. One part alkali activated materials: A state-of-the-art review. *J. Build. Eng.* **2022**, *57*, 104871.
15. Siddique, R.; Klaus, J. Influence of metakaolin on the properties of mortar and concrete: A review. *Appl. Clay Sci.* **2009**, *43*, 392–400.
16. Alexander, M.G.; Jaufeerally, H.; Mackechnie, J.R. Structural and durability properties of concrete made with Corex slag. *Dep. Civ. Eng. UCT Res. Monog.* **2003**, *6*, 30.
17. Luukkonen, T.; Abdollahnejad, Z.; Yliniemi, J.; Kinnunen, P.; Illikainen, M. One-part alkali-activated materials: A review. *Cem. Concr. Res.* **2018**, *103*, 21–34.
18. Wang, Y.S.; Alrefaei, Y.; Dai, J.G. Roles of hybrid activators in improving the early-age properties of one-part geopolymer pastes. *Constr. Build. Mater.* **2021**, *306*, 124880.
19. Granizo, M.L.; Alonso, S.; Blanco-Varela, M.T.; Palomo, A. Alkaline activation of metakaolin: Effect of calcium hydroxide in the products of reaction. *J. Amer Cer Socie* **2002**, *85*, 225–231.
20. Kim, B.; Lee, S.; Chon, C.M.; Cho, S. Setting behaviour and phase evolution on heat treatment of metakaolin-based geopolymers containing calcium hydroxide. *Materials* **2022**, *15*, 194.
21. Tan, H.; Zou, F.; Liu, M.; Ma, B.; Guo, Y.; Jian, S. Effect of the adsorbing behaviour of phosphate retarders on hydration of cement paste. *J. Mater. Civ. Eng.* **2017**, *29*, 4017088.
22. Sood, D.; Hossain, K.M.A. Strength, shrinkage and early age characteristics of one-part alkali-activated binders with high-calcium industrial wastes, solid reagents and fibers. *J. Comp. Sci.* **2021**, *5*, 315.
23. Chang, J.J. A study on the setting characteristics of sodium silicate-activated slag pastes. *Cem. Concr. Res.* **2003**, *33*, 1005–1011.
24. Zhang, T.; Ma, B.; Tan, H.; Qi, H.; Shi, T. Effect of sodium carbonate and sodium phosphate on hydration of cement paste. *J. Build. Eng.* **2022**, *45*, 103577.
25. Yeheyis, M.; Hewage, K.; Alam, M.S.; Eskicioglu, C.; Sadiq, R. An overview of construction and demolition waste management in Canada: A lifecycle analysis approach to sustainability. *Clean. Tech. Env. Pol.* **2013**, *15*, 81–91.
26. Benachio, G.L.F.; Freitas, M.D.C.D.; Tavare, S.F. Circular economy in the construction industry: A systematic literature review. *J. Clean. Prod.* **2020**, *260*, 121046.
27. Geyer, R.; Jambeck, J.R.; Law, K.L. Production, use, and fate of all plastics ever made. *Sci. Advan* **2017**, *3*, e1700782.
28. Thorneycroft, J.; Orr, J.; Savoikar, P.; Ball, R.J. Performance of structural concrete with recycled plastic waste as a partial replacement for sand. *Constr. Build. Mater.* **2018**, *161*, 63–69.
29. El-Seidy, E.; Sambucci, M.; Chougan, M.; Al-Kheetan, M.J.; Biblioteca, I.; Valente, M.; Ghaffar, S.H. Mechanical and physical characteristics of alkali- activated mortars incorporated with recycled polyvinyl chloride and rubber aggregates. *J. Build. Eng.* **2022**, *60*, 105043.
30. Arjomandi, A.; Mousavi, R.; Tayebi, M.; Nematzadeh, M.; Gholampour, A.; Aminian, A.; Gencel, O. The effect of sulfuric acid attack on mechanical properties of steel fiber-reinforced concrete containing waste nylon aggregates: Experiments and RSM-based optimisation. *J. Build. Eng.* **2022**, *64*, 105500.

31. South Africa-State of Waste Report II. A Report on the State of Waste in South Africa. 2018. Available online: www.environment.gov.za (access on 6 July 2023).
32. Hajimohammadi, A.; Ngo, T.; Kashani, A. Glass waste versus sand as aggregates: The characteristics of the evolving geopolymer binders. *J. Clean. Prod.* **2018**, *193*, 593–603.
33. Gholampour, A.; Danish, A.; Ozbakkaloglu, T.; Yeon, J.H.; Gencel, O. Mechanical and durability properties of natural fiber-reinforced geopolymers containing lead smelter slag and waste glass sand. *Constr. Build. Mater.* **2022**, *352*, 129043.
34. Steyn, Z.C.; Babafemi, A.J.; Fataar, H.; Combrinck, R. Concrete containing waste recycled glass, plastic and rubber as sand replacement. *Constr. Build. Mater.* **2021**, *269*, 121242.
35. *ASTM C618-08a*; Standard specification for coal fly ash and raw or calcined natural pozzolan for use in concrete. ASTM International: West Conshohocken, PA, USA, 2008.
36. Burciaga-Díaz, O.; Escalante-García, J.I. Structural transition to well-ordered phases of NaOH-activated slag-metakaolin cements aged by 6 years. *Cem. Concr. Res.* **2022**, *156*, 106791.
37. Davidovit, U.S. Patent No. 4,349,386. Washington DC: U.S. Patent and Trademark Office, 1982.
38. Davidovit, U.S. Patent No. 4,472,199. Washington DC: U.S. Patent and Trademark Office, 1984.
39. Yang, K.H.; Song, J.K.; Lee, J.S. Properties of alkali-activated mortar and concrete using lightweight aggregates. *Mater. Struct.* **2010**, *43*, 403–416.
40. Raj, N.; Patil, S.G.; Bhattacharjee, B. Concrete Mix Design by Packing Density Method. *IOSR J. Mech. Civ. Eng.* **2014**, *11*, 34–46.
41. Kanagaraj, B.; Anand, N.; Alengaram, U.J.; Praveen, B.; Tattukolla, K. Performance evaluation on engineering properties and sustainability analysis of high strength geopolymer concrete. *J. Build. Eng.* **2022**, *60*, 105147.
42. Cimbala, J.M. *Taguchi Orthogonal Arrays*; Pennsylvania State University: State College, PA, USA, 2014; pp. 1–3.
43. Wang, K.T.; Du, L.Q.; Lv, X.S.; He, Y.; Cui, X.M. Preparation of drying powder inorganic polymer cement based on alkali-activated slag technology. *Powder Technol.* **2017**, *312*, 204–209.
44. Kuo, W.T.; Wang, H.Y.; Shu, C.Y. Engineering properties of cementless concrete produced from GGBFS and recycled desulfurisation slag. *Const. Build. Mater.* **2014**, *63*, 189–196.
45. Nath, P.; Sarker, P.K. Effect of GGBFS on setting, workability and early strength properties of fly ash geopolymer concrete cured in ambient condition. *Constr. Build. Mater.* **2014**, *66*, 163–171.
46. *EN 196-3:2016*; Methods of Testing Cement–Part 3: Determination of Setting Times and Soundness. British Standard Institution: London, UK, 2016.
47. *BS EN 12350-2: 2019*; Testing Fresh Concrete. British Standard Institution: London, UK, 2019.
48. *BS EN 12390-7: 2019*; Testing Hardened Concrete Density. British Standard Institution: London, UK, 2019.
49. *BS EN 12390-1: 2021*; Testing Hardened Concrete Shape, Dimensions and other Requirements for Specimens and Moulds. British Standard Institution: London, UK, 2021.
50. *BS EN 12390-2, 2019*; Testing Hardened Concrete Making and Curing Specimens for Strength Tests. British Standard Institution: London, UK, 2019.
51. *BS EN 12390-6: 2009*; Testing Hardened Concrete Tensile Splitting Strength of Test Specimens. British Standard Institution: London, UK, 2009.
52. *ASTM C469-02*; Standard Test Method for Static Modulus of Elasticity and Poisson's Ratio of Concrete in Compression. ASTM International: West Conshohocken, PA, USA, 2002.
53. Gong, C.; Yang, N. Effect of phosphate on the hydration of alkali-activated red mud-slag cementitious material. *Cem. Concr. Res.* **2000**, *30*, 1013–1016.
54. Ling, T.C.; Poon, C.S.; Kou, S.C. Influence of recycled glass content and curing conditions on the properties of self-compacting concrete after exposure to elevated temperatures. *Cem. Concr. Compos.* **2012**, *34*, 265–272.
55. Malik, M.I.; Bashir, M.; Ahmad, S.; Tariq, T.; Chowdhary, U. Study of concrete involving use of waste glass as partial replacement of fine aggregates, *IOSR J. Eng.* **2013**, *7*, 8–13.
56. Sharifi, Y.; Houshiar, M.; Aghebati, B. Recycled glass replacement as fine aggregate in self-compacting concrete. *Front. Struct. Civ. Eng.* **2013**, *7*, 419–428.
57. Wu, J.-Q.; Li, B.; Chen, Y.-T.; Ghiassi, B. Investigation on the roles of glass sand in sustainable engineered geopolymer composites. *Constr. Build. Mater.* **2023**, *363*, 129576.
58. Adamu, M.; Trabanpruek, P.; Jongvivatsakul, P.; Likitlersuang, S.; Iwanami, M. Mechanical performance and optimisation of high-volume fly ash concrete containing plastic wastes and graphene nanoplatelets using response surface methodology, Construct. Build. *Mater*ials **2021**, *308*, 125085.
59. Haruna, S.; Jongvivatsakul, P.; Hamcumpai, K.; Iqbal, H.W.; Nuaklong, P.; Likitlersuang, S.; Iwanam, M. Multiscale investigation of the impact of recycled plastic aggregate as a fine aggregate replacement on one-part alkali-activated mortar performance. *J. Build. Eng.* **2024**, *86*, 108768.
60. Iucolano, F.; Liguori, B.; Caputo, D.; Colangelo, F.; Cioffi, R. Recycled plastic aggregate in mortars composition: Effect on physical and mechanical properties. *Mater. Des.* **2013**, *52*, 916–922.
61. Silva, G.; Kim, S.; Aguilar, R.; Nakamatsu, J. Natural fibers as reinforcement additives for geopolymers–A review of potential eco-friendly applications to the construction industry. *Sust. Mater. Technol.* **2020**, *23*, e00132.
62. Babafemi, A.J.; Šavija, B.; Paul, S.C.; Anggraini, V. Engineering properties of concrete with waste recycled plastic: A review. *Sustainability* **2018**, *10*, 3875.

63. Ajayi, B.L.; Babafemi, A.J. Performance of slag-metakaolin-based geopolymer concrete (GPC) with recycled plastic eco-aggregate. In Proceedings of the Young Concrete Researchers, Engineers & Technologists, Stellenbosch, South Africa, 12–14 July 2023.
64. Hajimohammadi, A.; Ngo, T.; Kashani, A. Sustainable one-part geopolymer foams with glass fines versus sand as aggregates. *Constr. Build. Mater.* **2018**, *171*, 223–231.
65. Tayeh, B.A.; Almeshal, I.; Magbool, H.M.; Alabduljabbar, H.; Alyousef, R. Performance of sustainable concrete containing different types of recycled plastic. *J. Clean. Prod.* **2021**, *328*, 129517.
66. Gu, V.; Ozbakkaloglu, T. Use of recycled plastics in concrete: A critical review. *Waste Manag.* **2016**, *51*, 19–42.
67. Sharma, R.; Bansal, P.P. Use of different forms of waste plastic in concrete—A review. *J. Clean. Prod.* **2016**, *112*, 473–482.
68. Almeshal, I.; Tayeh, B.A.; Alyousef, R.; Alabduljabbar, H.; Mohammed, A.M.; Alaskar, A. Use of recycled plastic as fine aggregate in cementitious composites: A review. *Constr. Build. Mater.* **2020**, *253*, 119146.
69. El-Seidy, E.; Sambucci, M.; Chougan, M.; Al-Noaimat, Y.A.; Al=Kheetan, M.J.; Bibliteca, I.; Valente, M.; Ghaffar, S.H. Alkali activated materials with recycled unplasticised polyvinyl chloride aggregates for sand replacement. *Constr. Build. Mater.* **2023**, *409*, 134188.
70. Senhadji, Y.; Siad, H.; Escadeillas, G.; Benosman, S.B.; Chihaoui, R.; Mouli, M.; Lachemi, M. Physical, mechanical and thermal properties of lightweight composite mortars containing recycled polyvinyl chloride. *Construct. Build. Mater.* **2019**, *195*, 198–207.
71. Chen, W.; Dong, S.; Liu, Y.; Liang, Y.; Skoczylas, E. Effect of waste glass as fine aggregate on properties of mortar. *Materials* **2022**, *15*, 8499.
72. Borek, K.; Czapik, P.; Dachowski, R. Recycled glass as a substitute for quartz sand in silicate products. *Materials* **2020**, *13*, 1030.
73. Davidovits, J. Geopolymer cement: A review. *Geopolymer Inst. Tech. Pap.* **2013**, *21*, 1–11.
74. Huseien, G.F.; Mirza, J.; Ismail, M.; Hussin, M.W. Influence of different curing temperatures and alkali activators on properties of GBFS geopolymer mortars containing fly ash and palm-oil fuel ash. *Constr. Build. Mater.* **2016**, *125*, 1229–1240.
75. Luo, Y.; Bao, S.; Zhang, Y.; Yuan, Y. Recycling vanadium-bearing shale leaching residue for the production of one-part geopolymers. *Mater. Res. Express* **2019**, *6*, 105203.
76. Xiao, R.; Ma, Y.; Jiang, X.; Zhang, M.; Zhang, Y.; Wang, Y.; Huang, B.; He, Q. Strength, microstructure, efflorescence behavior and environmental impacts of waste glass geopolymers cured at ambient temperature. *J. Clean. Prod.* **2020**, *252*, 119610.
77. Ge, Z.; Sun, R.; Zhang, K.; Gao, Z.; Li, P. Physical and mechanical properties of mortar using waste polyethylene terephthalate bottles. *Constr. Build. Mater.* **2013**, *44*, 81–86.
78. Babafemi, A.J.; Sirba, N.; Paul, S.C.; Miah, M.J. Mechanical and durability assessment of recycled waste plastic (Resin8 & PET) eco-aggregate concrete. *Sustainability* **2022**, *14*, 5725.
79. Gagg, C.R. Cement and concrete as an engineering material: An historic appraisal and case study analysis. *Eng. Fail. Anal.* **2014**, *40*, 114–140.
80. Hannawi, K.; Kamali-Bernard, S.; Prince, W. Physical and mechanical properties of mortars containing PET and PC waste aggregates. *Waste Manag.* **2010**, *30*, 2312–2320.
81. Azhdarpour, A.M.; Nikoudel, M.R.; Taheri, M. The effect of using polyethylene terephthalate particles on physical and strength-related properties of concrete; A laboratory evaluation. *Constr. Build. Mater.* **2016**, *109*, 55–62.
82. Choi, Y.W.; Moon, D.J.; Chung, J.S.; Cho, S.K. Effects of waste PET bottles aggregate on the properties of concrete. *Cem. Concr. Res.* **2005**, *35*, 776–781.
83. *ACI 318M-14*; Building Code Requirements for Structural Concrete (ACI 318-14) and Commentary (ACI 318R-14). An American Concrete Institute: Farmington Hills, MI, USA, 2014.
84. *EN 1992-1-1: 2004*; Design of Concrete Structures—Part 1-1: General rules and rules for buildings. European Standard: Brussels, Belgium, 2004.
85. Batayneh, M.; Marie, I.; Asi, I. Use of selected waste materials in concrete mixes. *Waste Manag.* **2007**, *27*, 1870–1876.
86. Aciu, C.; Ilutiu-Varvara, D.A.; Manea, D.L.; Orban, Y.A.; Babota, F. Recycling of plastic waste materials in the composition of ecological mortars. *Procedia Manuf.* **2018**, *22*, 274–279.
87. Kou, S.C.; Lee, G.; Poon, C.S.; Lai, W.L. Properties of lightweight aggregate concrete prepared with PVC granules derived from scraped PVC pipes. *Waste Manag.* **2009**, *29*, 621–628.